

NON-INVASIVE GRADING TECHNIQUE FOR RUBY GEMSTONE USING CHARGE-COUPLED DEVICE (CCD)

Fatinah Mohd Rahalim, Juliza Jamaludin*, Syarfa Najihah Raisin

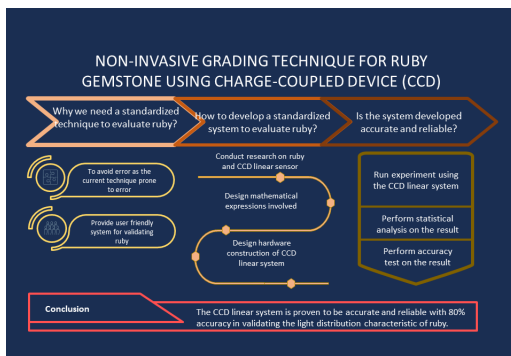
Faculty of Engineering and Built Environment, Universiti Sains Islam Malaysia, 71800 Bandar Baru Nilai, Negeri Sembilan, Malaysia

Article history

Received
03 February 2022
Received in revised form
28 April 2022
Accepted
18 May 2022
Published online
28 February 2023

*Corresponding author
juliza@usim.edu.my

Graphical abstract



Abstract

Ruby is one of the most popular and high-value gemstones that always attract the gemologist and jeweler in the diamond market. The wide use of ruby in various industries makes the grading of this gems more complicated due to a lot of synthetic and imitation rubies are made. The current grading techniques are mostly depending on the human visual assessment which prone to errors. This paper proposes a system that helps in grading the clarity characteristic of the ruby in non-invasive manner. The system includes a charge-coupled devices (CCD) and laser that is designed in the most suitable and effective way to conduct inspection on the light intensity of the ruby which will then determine the clarity of the ruby. CCD linear sensor is widely known as the reliable sensor especially when use in the optical system. The CCD linear sensor capture the light intensity from the ruby and convert it into the voltage value. The result shows a value of 1.7918 V obtained from the CCD linear sensor when ruby is placed in the system. This concludes that the CCD system can detect even slightest changes in the light intensity that can pass through the ruby and falls on the CCD linear sensor. The system is proven to be a reliable and effective system with 80% accuracy.

Keywords: Ruby, charge-coupled device (CCD), non-invasive, clarity, light intensity

© 2023 Penerbit UTM Press. All rights reserved

1.0 INTRODUCTION

Ruby is one of the most popular gemstones and have been cherished since long time ago [1]. It is from the class corundum, made of various chemical compound mainly the Iron (Fe) and Chromium (Cr) that make the color appear as red [2]. The ruby has widely been used as jewelry, laser and applied in various industries such as medical industries, jewelry industries and many more. Due to its significant optical properties, such as having high hardness (9 on Mohs scale), strong, have stable chemical and thermal properties, high insulation and optical transparency is an advantage for modern technological applications which is applied in lasers, optoelectronics, temperature sensors and precision machinery devices [3].

The grading of ruby is not as simple as grading the gold, silver, and bronze as it requires very detail inspection. The diamond trade system developed the grading system for diamond and colored stone which also include ruby based on 4Cs (color,

clarity, cut and carat weight) that is very important for market demand value [4]. Currently, there is no standardized grading technique for grading the ruby [5]. The current grading techniques are basically depending on the human eyes' inspection by the experienced gemmologist [2]. The International Gem Society stated that the must-have tools in the gemology laboratory are a loupe and microscope to magnify the gemstone, refractometer to measure the refractive index, birefringence, and optical characteristics of gemstones, dichroscope, polariscope, and spectroscope. These tools are usually used together with other miscellaneous tools, such as the jeweler's eyes, diamond detectors, and hardness sets [6].

In addition, the Gemology Tools Professional is a software that stores more than 500 databases of various gemstones in various properties [7]. These databases are used together with the human eyes' inspection to determine the grade of the gemstones. This current technique is prone to errors as it depends highly on the human visual inspection.

Since the ruby is very hard to be found, synthetic rubies are also made in laboratories [8]. This leads to more complicated grading process as the synthetic rubies made are almost similar to the original rubies extracted from the Earth. The gemologist had a harder time in determining the ruby grade due to this situation. To improve the current grading technique, a new quantitative grading technique is proposed. A charge-coupled device (CCD) linear sensor is used that provides non-invasive grading inspection [9] to the ruby as it does not need to disturb the internal composition of the ruby physically and chemically. The CCD linear sensor analyze the light distribution characteristic of the ruby and convert the light intensity value into voltage value. This paper provides a brief overview on the non-invasive grading technique for ruby gemstone by using CCD linear sensor.

The CCD linear sensor have been widely used in various industries especially in industries that involves optical system [10]. The astronomy, photography, medical, scanners and many more used the CCD as the sensor as it provides high resolution photos, low noise, and also low power. CCD is applied in telescope, cameras, scanners, X-ray computed tomography (CT), MRI scanner and many more [10, 11, 12, 13, 14]. Furthermore, CCD sensor is also very competent in detecting transparency of objects according to the experiment conducted by previous researchers [11, 12, 13].

To do inspections on gems, the steps involved are analyzing the chemical composition, determining the natural or synthetic gems, screening for enhancing treatments, grading and sometimes involves determining their geographic origin [14]. All the data should be retrieved by using non-invasive and non-destructive procedures to avoid destroying and damaging the gems.

Since the CCD linear sensor is a sensor that is very sensitive to light [15, 16, 17, 18], this sensor is the most suitable sensor to analyze the light distribution in the ruby. CCD linear sensor is best combined with the laser because it provides exact accuracy, high sensitivity and reading distance stability [13, 19]. The concept of this research is by analyzing the clarity of the ruby based on how much light can pass through it using CCD linear sensor.

This research analyzes the characteristic of light distribution in rubies for grading valuation. The experiment is set up in an optimal condition for the CCD linear sensor to work efficiently. The temperature, light intensity, and input voltage source of the CCD linear sensor are the main conditions needed to be maintained at the optimum condition so that the CCD linear sensor does not become saturated and produce undesirable results. Simulations and experiments have been developed to investigate the light intensity received by the CCD linear sensor from the ruby. The light propagation conditions involved in this research—light reflection and absorption—are analyzed mathematically using the LabVIEW software. Then, the light intensity data received by the sensor, which is represented by the CCD output voltage, is statistically analyzed using the Minitab software. These data determine the clarity of the ruby.

2.0 METHODOLOGY

Essentially, a suitable environment is prepared to prevent the CCD linear sensor from being saturated. The CCD linear sensor requires relative humidity to be within 65%–85% and the

temperature to be within 25°C–33°C [18]. Similarly, the laser is maintained at 0.5 lux for optimum CCD linear sensor working conditions [16]. The CCD system is designed in a dark area where the laser is beamed towards the CCD linear sensor and the ruby is placed in between the laser and the CCD linear sensor. The dark area is maintained at the minimum external light to enhance the accuracy of the CCD so that the CCD receives the highest intensity of light from the ruby.

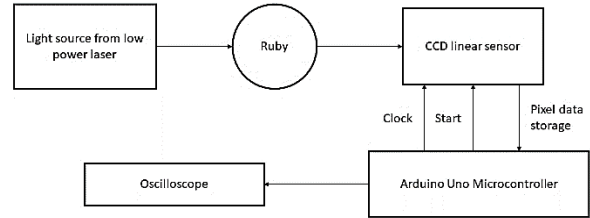


Figure 1 Block diagram of CCD linear system to inspect the ruby

The overall block diagram of the CCD system is shown in Figure 1. As the laser is beamed towards the CCD linear sensor and passes through the ruby, the light from the ruby will fall onto the CCD linear sensor. The CCD linear sensor analyze the light received and convert the amount of light captured into a voltage value. The Arduino Uno Microcontroller is used to design the system. The final voltage value is displayed on the oscilloscope.

The mathematical modelling for the light reflectance and light attenuation are developed first to obtain the theoretical light intensity of the ruby. Light reflectance is considered in this experiment as the light from laser may be reflected away once it hits the ruby surface. While the light absorbance is the light that successfully pass the ruby [20, 21].

Light Reflectance

Light reflectance is considered as energy loss as the light is reflected away from the ruby. The reflected light will not be the effective light and will be excluded from the finalized data from the CCD linear sensor [17, 21].

$$I_{final\ reflectance} = I_i - \left[I_i \left(\frac{n_2 - n_1}{n_2 + n_1} \right)^2 \right] \quad (1)$$

The final light reflectance is represented by the above equation 1 where the I_i is the initial light reflectance, n_1 is the transmitted refractive index and n_2 is the incident refractive index. As the incident angle of the incident ray increases, more light is reflected resulting in the reducing amount of light emitted through the ruby. The light reflectance equation is simulated in the LabVIEW software as in Figure 2.

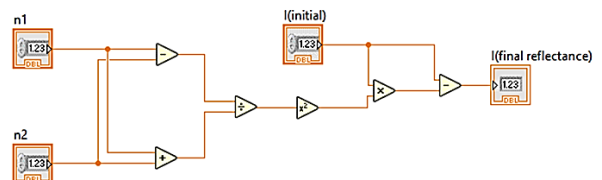


Figure 2 LabVIEW simulation of the light reflectance equation

Light Attenuation

Another situation involved in this experiment is the light attenuation. The light is attenuated or absorbed into the ruby when the light pass through the ruby. the light attenuation is represented by the following equation 2.

$$I_{out} = I_{in}e^{-\alpha x} \tag{2}$$

Where α is the linear attenuation coefficient and x is the distance of the light traversed. The attenuated light is the effective light that will be analyzed. Light is attenuated and converted into energy when passing through the ruby. Along the optical path, the output light intensity is attenuated exponentially according to the Beer-Lambert Law [17, 21]. The LabVIEW simulation for the light attenuation equation is shown in the Figure 3 below.

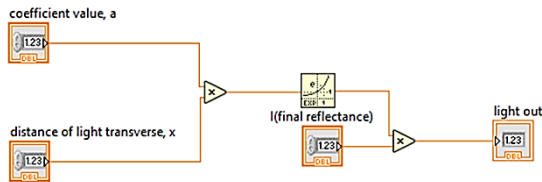


Figure 3 LabVIEW simulation of the light attenuation equation

The final voltage value obtained from the mathematical modelling simulation involving both light reflectance and light attenuation is 1.9941 V. The theoretical voltage value is then compared with the actual voltage value obtained from the experiment.

The experiment is set up in a dark condition as in Figure 4. As shown in the Figure 4, the red laser is beamed towards the CCD linear sensor and the ruby is placed just above the CCD linear sensor. The light from the laser that pass through the ruby is then fall onto the CCD linear sensor. The CCD linear sensor analyses the light intensity received and convert it into voltage value. The data of the voltage value is shown on the oscilloscope.

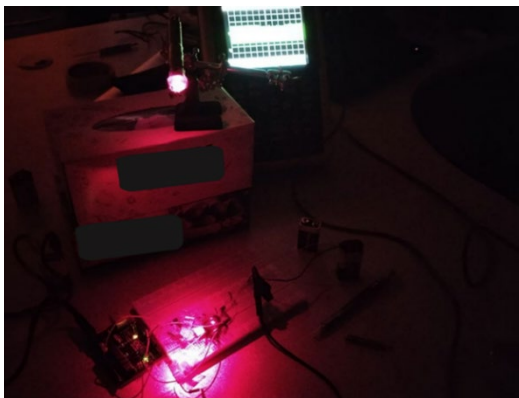


Figure 4 Experimental setup of CCD linear sensor system in dark condition

3.0 RESULTS AND DISCUSSION

A number of 600 data for each condition are taken into consideration and the mean data of each condition is analyzed.

The reference voltage is taken when the experiment is conducted in the laser on and off condition when the ruby is not in the system. The reference voltage is used as the reference point for the data when the ruby present in the system. The voltage in the Table 1 is the reference voltages taken in the laser on and off condition without ruby in the system.

Table 1 The CCD voltage output and light intensity in the laser condition off and on

Condition of Laser	CCD Voltage Output (V)	Light Intensity (lx)
Off	4.282	0
On	1.583	1

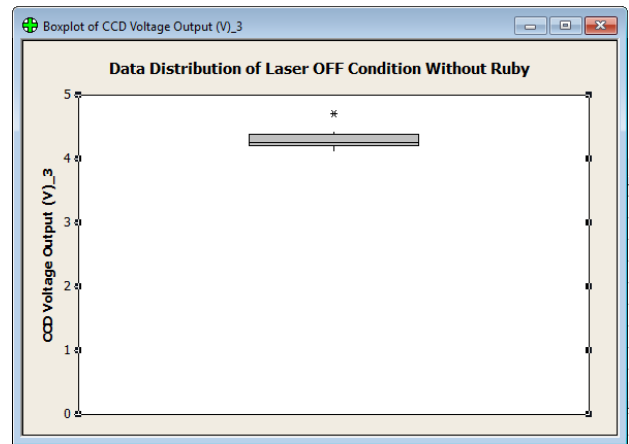


Figure 5 Data distribution of CCD output voltage on laser off condition

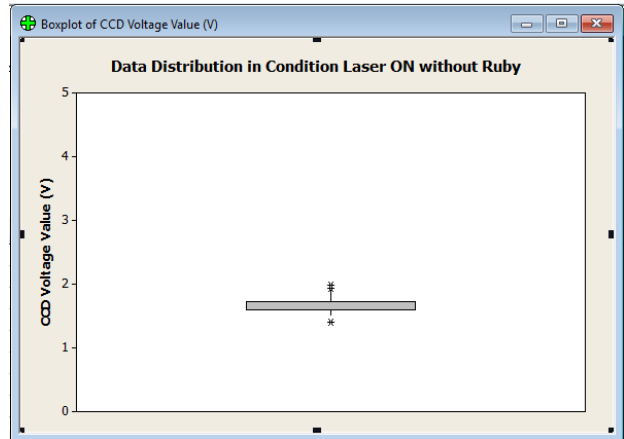


Figure 6 Data distribution of CCD output voltage on laser on condition

Figure 5 and Figure 6 show the distribution of data in the laser off and on condition respectively. From the data obtained, it can be concluded that the CCD linear sensor executes higher voltage value in dark condition or low light intensity. Otherwise, when the CCD linear sensor detect higher light intensity, the voltage executed is lower.

The intensity of the laser is proportional directly to the CCD output voltage. The graph in Figure 7 represents the voltage output of the CCD versus the light intensity of the laser. Based on this graph, it can be presumed that the CCD voltage output is inversely proportional to the intensity of the laser with a -2.6983 gradient and an interception value of 4.2817 with a zero-light

intensity. The following equation 3 interprets the relationship between the CCD voltage output and the light intensity.

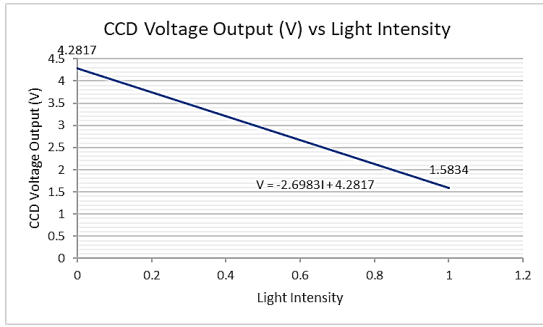


Figure 7 The graph of CCD voltage output against light intensity

$$V = -2.6983I + 4.2817 \quad (3)$$

The same procedure is done in the condition where the ruby appear in the system. This procedure involves the condition where light propagates from air into the ruby. This situation involves the ratio of refractive index between air and ruby as the light travels from air into the ruby. The incoming light intensity (*I*) is reduced at the first surface of the ruby due to the reflection at the air and ruby interface.

The Table 2 shows the theoretical value of the light intensity and the theoretical CCD voltage output gained by using the equation 1, equation 2 and equation 3.

Table 2 The CCD voltage output and light intensity in the air-to-ruby light propagation

Condition of light propagation	CCD Voltage Output (V)	Light Intensity (Ix)
Air/Ruby	1.9941	0.8478

When ruby is in the system with laser in an OFF condition, the data show a slightly lower voltage value, as shown in Figure 8. This indicates that the ruby itself produces its own fluorescent light due to the reduction of chromium and the presence of iron, as mentioned by previous researchers [22]. Furthermore, this situation also proves that the CCD can detect even small changes of light intensity in the system [23]. The box plot in Figure 8 shows the distribution of CCD voltage value when ruby is in the system with laser condition OFF.

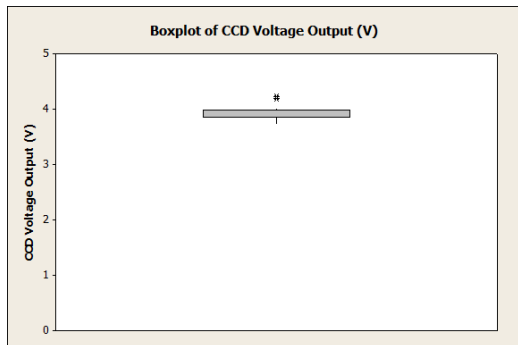


Figure 8 Data distribution of CCD output voltage on laser off condition with the presence of ruby in the system

In the condition where the laser is ON, the data shows a much lower value of the CCD output voltage as in Figure 9. This implies that the CCD linear sensor receives much more light intensity since the laser is in ON condition. The box plot in Figure 8 shows the data distribution of CCD output voltage when a ruby is present in the system with laser ON condition.

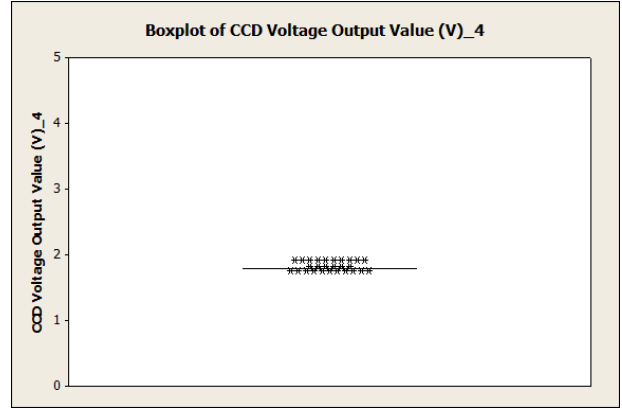


Figure 9 Data distribution of CCD output voltage on laser on condition with the presence of ruby in the system

According to the Minitab 16 software, the best way to prove that the means of two samples, whether they are significantly differing, is by using a 2-sample t-test. In this experiment, the mean of ruby's presence in the system is compared with the mean of ruby's absence in the system in both laser off and on conditions. So, the 2-sample t-test is the best technique to analyze the data.

Figure 10 shows the t-test for the mean sample of data in the condition of laser off with the presence and absence of ruby. The null hypothesis for this t-test is that the mean CCD voltage output value when the ruby is not in the system in the laser OFF condition is equal to the mean CCD voltage output value when the ruby is in the system in the laser off condition. Alternatively, the alternative hypothesis for this t-test is that the mean CCD voltage output value when the ruby is not in the system in the laser off condition is not equal to the mean CCD voltage output value when the ruby is in the system in the laser off condition.

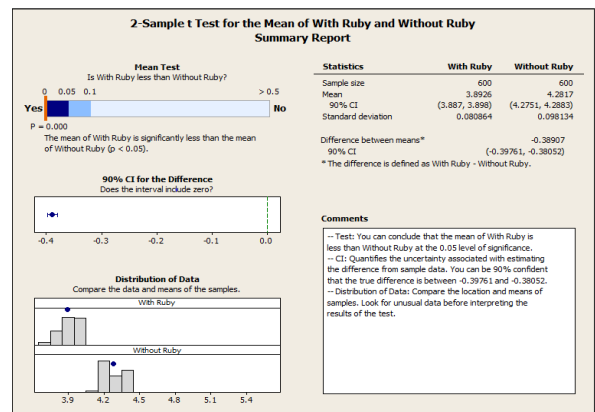


Figure 10 Summary of T-test on the laser condition off with and without ruby in the system

From the t-test summarized in Figure 10, it can be concluded that the mean of data with the ruby is lower than the mean data

obtained without the ruby with a 0.05 level of significance. Hence, the null hypothesis is rejected as the P-value is less than 0.05. Confidence intervals give a range of values that the result occurs within the population. The t-test above shows a 90% confidence level with the confidence intervals of different values between the data with ruby and without ruby is in the range of 0.3976 and 0.3805. This means that when the experiment is repeated, 90% of the time, this result will occur.

Figure 11 represent the t-test result that summarize the data obtained from the CCD linear sensor system in the condition of laser on with and without ruby in the system. The null hypothesis for this t-test is that the mean data of the CCD voltage output in the laser on condition with the ruby in the system is equal to the mean data of the CCD voltage output in the laser on condition without the ruby. Whereby the alternative hypothesis is that the mean data of the CCD voltage output in the laser on condition with the ruby in the system is unequal to the mean data of the CCD voltage output in the laser on condition without the ruby.

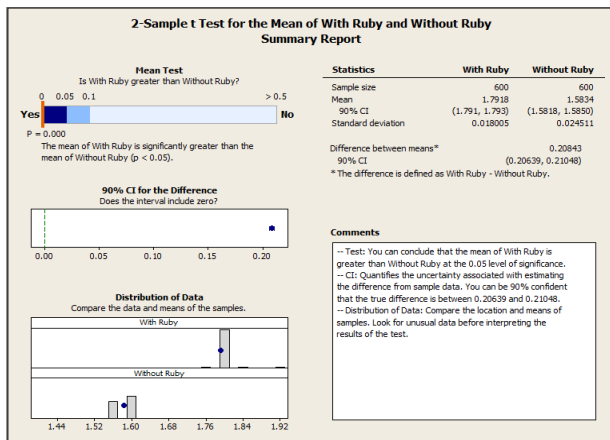


Figure 11 Summary of T-test on the laser condition on with and without ruby in the system

From the t-test summarized in Figure 11 it can be concluded that the mean of data with the ruby is significantly higher than the mean of data without the ruby with a 0.05 level of significance. Hence, the alternative hypothesis is accepted because the P-value is less than 0.05. The t-test above shows a 90% confidence level with the confidence intervals of difference value between the data with ruby and without ruby is in the range of 0.2064 and 0.2105. This means that when the experiment is repeated, 90% of the times this result will occur and the difference value between the condition with ruby and without ruby will fall in between the range 0.2064 and 0.2105.

Table 2 Theoretical and experimental value of CCD voltage output

Theoretical Value (V)	Experimental Value (V)
1.9941	1.7918

The accuracy test is conducted by comparing the theoretical and experimental value of the CCD voltage output using the accuracy formula as in equation 4. The system shows 80 percent of accuracy which means that the system is reliable on detecting the light intensity in ruby, hence it can also evaluate the clarity of the ruby.

$$\text{Relative accuracy, } A = 1 - \left| \frac{\text{Theoretical value} - \text{Experimental value}}{\text{Theoretical value}} \right|$$

$$\text{Relative accuracy, } A = 1 - \left| \frac{1.9941 - 1.7918}{1.9941} \right|$$

$$\text{Relative accuracy, } A = 0.7977$$

4.0 CONCLUSION

This research outlines a CCD system that results in a quantitative value of clarity characteristic of ruby specifically on the light intensity of the ruby. This method is non-invasive, which provides an advantage to the gemologists and gemstones appraisers as it will not disturb the internal composition of the ruby and does not damage the ruby. The CCD system, which consists of CCD linear sensor and laser is believed to be a reliable and compatible system that is helpful in the grading process of gemstones especially in ruby. The optimum condition prepared for the CCD linear sensor produced accurate result with 80% accuracy. The system also come out with a quantitative value, which is less prone to errors compared to the current techniques that mostly depend on the human vision. Hence, this system can help the gemologist and other people that is not specialized in gemology to analyze the clarity of the ruby in a more standardized and accurate method and help them in determining the ruby grades accurately. The CCD linear system is believed to be a reliable and accurate system in validating other gemstones because other gemstones also graded according to the 4Cs characteristics.

Acknowledgement

The authors would like to thank to Universiti Sains Islam Malaysia and ADS research group for their cooperation in this research paper. The research is supported by the Malaysian Ministry of Higher Education Fundamental Research Grant Nos. (FRGS/1/2020/WAB07/USIM/02/1) (USIM/FRGS/FKAB/KPT/53020).

References

- [1] Malsy, A. and Klemm, L. 2010. Distinction of Gem Spinel from the Himalayan Mountain Belt. *Chimia*. 64(10): 741-746. DOI: <https://doi.org/10.2533/chimia.2010.741>
- [2] Joseph, D., Lal, M., Shinde, P.S. and Padalia, B.D. 2000. Characterization of Gem Stones (Rubies and Sapphires) by Energy-Dispersive X-Ray Fluorescence Spectrometry. *X-Ray Spectrometry*. 29(2): 147-150. DOI: [https://doi.org/10.1002/\(SICI\)1097-4539\(200003/04\)29:2<147:AID-XRS370>3.0.CO;2-K](https://doi.org/10.1002/(SICI)1097-4539(200003/04)29:2<147:AID-XRS370>3.0.CO;2-K)
- [3] Liu, F., Goodman, B.A., Tan, X., Wang, X., Chen, D. and Deng, W. 2019. Luminescence and EPR Properties of High Quality Ruby Crystals Prepared by the Optical Floating Zone Method. *Optical Materials*. 91: 183-188. DOI: <https://doi.org/10.1016/j.optmat.2019.03.018>
- [4] Giuliani, G., Groat, L.A., Fallick, A.E., Pignatelli, I. and Pardieu, V. 2020. Ruby Deposits: A Review and Geological Classification. *Minerals*. 10(7): 597. DOI: <https://doi.org/10.3390/min10070597>
- [5] Brazeal, B. 2019. Central Asian Crypto-Jews in the Global Emerald Economy. *The Extractive Industries and Society*. 6(4): 1047-1054. DOI: <https://doi.org/10.1016/j.exis.2019.03.014>

- [6] Karampelas, S., Kiefert, L., Bersani, D. and Vandenabeele, P. 2020. Gems and Gemmology. DOI: <https://doi.org/10.1007/978-3-030-35449-7>
- [7] Gemology Tools Professional, Retrieved from <https://gemologytools.com/>
- [8] Sahoo, R.K., Singh, S.K. and Mishra, B.K. 2016. Surface and Bulk 3D Analysis of Natural and Processed Ruby Using Electron Probe Micro Analyzer and X-Ray Micro CT Scan. *Journal of Electron Spectroscopy and Related Phenomena*. 211: 55-63. DOI: <https://doi.org/10.1016/j.elspec.2016.06.004>
- [9] Raisin, S.N., Jamaludin, J., Ismail, I., Balakrishnan, S.R., Sahrim, M., Naeem, B., Mohamad, F.A.J., Zain, A.S.M. and Fauzi, A.S.M. 2020. A Study of Object Transparency Via Charge-Coupled Device Mathematical Modelling Assessment. *Malaysian Journal of Science Health & Technology*. 7. DOI: <https://doi.org/10.33102/mjosht.v7i.115>
- [10] Mukherjee, S. 2011. Applied Mineralogy: Applications in Industry and Environment. DOI: <https://doi.org/10.1007/978-94-007-1162-4>
- [11] Liao, K.W., Lu, K.J., Luo, R.C. and Yeh, J.A. 2016. Portable Dielectric Tunable Forensic Lens Design for Jadeite Analysis. *2016 International Conference on Optical MEMS and Nanophotonics (OMN)*. DOI: <https://doi.org/10.1109/OMN.2016.7565889>
- [12] Mehta, S., Patel, A. and Mehta, J. 2015. CCD or CMOS Image Sensor for Photography. *2015 International Conference on Communications and Signal Processing (ICCSP)*. DOI: <https://doi.org/10.1109/ICCSP.2015.7322890>
- [13] Luo, B., Huo, J., Chen, Y., Li, B. and Luo, J. 2018. XCR4C: A Rad-Hard Full-Function CDS ASIC for X-Ray CCD Applications. *2018 IEEE Nuclear Science Symposium and Medical Imaging Conference Proceedings (NSS/MIC)*. DOI: <https://doi.org/10.1109/NSSMIC.2018.8824616>
- [14] Ahline, N. 2020. Staurolite in a Mozambique Ruby. *Gems & Gemology*. 56(3): 434-435.
- [15] Jamaludin, J., Rahim, R.A., Rahiman, M.H.F. and Rohani, J.M. 2019. CCD Optical Tomography System to Detect Solid Contamination in Crystal-Clear Water. *IEEE Transactions on Industrial Electronics*. 67(4): 3248-3256. DOI: <https://doi.org/10.1109/TIE.2019.2908589>
- [16] Jamaludin, J., Rahim, R.A., Rahim, H.A., Rahiman, M.H.F., Muji, S.Z.M. and Rohani, J.M. 2016. Charge Coupled Device Based on Optical Tomography System in Detecting Air Bubbles in Crystal Clear Water. *Flow Measurement and Instrumentation*. 50: 13-25. DOI: <https://doi.org/10.1016/j.flowmeasinst.2016.06.001>
- [17] Rahalim, F.M., Jamaludin, J., Raisin, S.N., Ismail, I., Wahab, Y.A., Rahim, R.A., Balakrishnan, S.R., Ismail, W.Z.W., Mohamad, F.A.J. and Zaini, N.A.H.S. 2021. Analysis on Clarity of Rubies Gemstones Using Charge-Coupled Device (CCD). *Journal of Tomography System & Sensors Application*. 4(1): 80-84. DOI: <https://oarep.usim.edu.my/jspui/handle/123456789/13330>
- [18] Jamaludin, J., Rahim, R.A., Rahiman, M.H.F., Wahab, Y.A., Rohani, J.M., Sahrim, M., Ismail, W.Z.W., Ismail, I. and Balakrishnan, S.R. 2018. Optical Tomography System Using Charge-Coupled Device for Transparent Object Detection. *International Journal of Integrated Engineering*. 10(4): 105-108. DOI: <https://doi.org/10.30880/ijie.2018.10.04.017>
- [19] Jamaludin, J., Rahim, R.A., Rahim, H.A., Rahiman, M.H.F., Muji, S.Z.M., Jumaah, M.F., Fadzil, N.S.M., Ahmad, N., Sahlan, S., Ahmad, A., Yunus, Y. and Abas, K.H. 2015. Analysis on the Performance of LED and Laser Diode with Charge Coupled Device (CCD) Linear Sensor Measuring Diameter of Object. *Jurnal Teknologi*. 77(17). DOI: <https://doi.org/10.11113/jt.v77.6418>
- [20] Durmuş, H.O., Kocaata, S., Naz, G., Çelik, Y.E., Çetin, E., Karaböce, B. and Seyidov, M.Y. 2004. Investigation of Basic Optical Properties of Tissue Phantoms under 635 nm Low-Level Laser Irradiation. *2020 IEEE International Symposium on Medical Measurements and Applications (MeMeA)*. DOI: <https://doi.org/10.1109/MeMeA49120.2020.9137206>
- [21] Idroas, M. 2004. A Charge Coupled Device Based Optical Tomographic Instrumentation System for Particle Sizing.
- [22] Chapin, M., Pardieu, V. and Lucas, A. 2015. Mozambique: A Ruby Discovery for the 21st Century. *Gems & Gemology*. 51(1): 44-54. DOI: <https://doi.org/10.5741/GEMS.51.1.44>
- [23] Jamaludin, J., Rahim, R.A., Rahim, H.A., Rahiman, M.H.F., Rohani, J.M. and Muji, S.Z.M. 2017. Charge-Coupled Device Based on Optical Tomography System in Detecting Solid and Transparent Objects in Non-Flowing Crystal Clear Water. *Optik*. 131: 813-825. DOI: <https://doi.org/10.1016/j.ijleo.2016.11.196>